Bifurcations in the hydrogen atom in the presence of a circularly polarized microwave field and a static magnetic field

V. Lanchares
Departamento de Matemáticas y Computación, Universidad de La Rioja, 26004 Logroño, Spain

M. Iñarrea and J. P. Salas
Area de Física Aplicada, Universidad de La Rioja, 26004 Logroño, Spain

(Received 10 February 1997)

In a classical model, the dynamics of the hydrogen atom subjected to a circularly polarized microwave field and a magnetic field is shown to belong to the family of so-called biparametric quadratic Hamiltonians. The energy-level structure is studied in terms of the parametric bifurcations. [S1050-2947(97)05209-8]

PACS number(s): 32.60.+i, 03.65.Sq, 02.90.+p

I. INTRODUCTION

As Lee, Brunello, and Farrelly show in [1], the dynamics of a hydrogen atom in the presence of a circularly polarized (CP) microwave field crossed with a magnetic field **B** (denoted as CP×**B**) presents two different behaviors. On the one hand, the electron can be confined in a region of space that includes the nucleus; on the other hand, it is possible to confine the electron, while moving on circularly Keplerian orbits, in a region of space that excludes the nucleus. The second behavior is because the fields are used to create, beyond the Stark saddle point, a minimum where stable motion can be maintained. Moreover, the problem treated in a reference frame rotating with the microwave field frequency resembles the quasi-Penning trap proposed in [2]; the depth of the well depends on the microwave field frequency and on the magnetic-field strength.

In this paper, and solely from the standpoint of classical mechanics, we study the CP×**B** problem when the electron is located near the nucleus, that is to say, in a region interior to the Stark saddle point. The CP×**B** problem is a nonintegrable system with three degrees of freedom because only the energy is an integral. To simplify the discussion, we reduce our study to a planar [two-dimensional (2D)] model. However, even the planar model is nonintegrable and has two degrees of freedom.

We can regard the CP×**B** problem as a perturbed Keplerian system and apply to it the methods of celestial mechanics. Considering the relatively simple nature of the perturbations, a Lie transformation is sufficient to carry out a ''normalization.'' The Lie transformation [3–5] is easy to build if it is not carried out to excessively high orders. In the present case, it is carried out to the first order. From this procedure results a normalized Hamiltonian that admits a new integral: the Keplerian term (i.e., the principal quantum number n). Thus, after normalization, the planar CP×**B** problem becomes integrable. From this reduction, as Coffey *et al.* [6] and Deprit *et al.* [7] did for the quadractic Zeeman effect and for the Stark quadratic Zeeman effect, our task is to study the evolution of the phase flow, that is to say, the existence and stability analysis of the equilibria points, the possible parametric bifurcations between them, as well as their consequences in the energy-levels structure.

The paper is organized as follows: Section II is dedicated to defining the problem and then, by means of a Delaunay normalization, an integrable approximation is obtained. By transforming the phase space of the normalized Hamiltonian to a two-dimensional sphere, the problem is shown to belong to the family of so-called biparametric quadratic Hamiltonians [8]. In Sec. III the stability of the equilibria, the bifurcations between them, and the phase flow evolution of the normalized Hamiltonian are analyzed. Finally, in Sec. IV the energy-level structure of the problem is studied.

II. HAMILTONIAN AND EQUILIBRIA

In atomic units, the Hamiltonian for the CP×**B** problem, in the dipole approximation, is given by

$$\mathcal{H}=\frac{1}{2}(P_x^2+P_y^2+P_y^2)-\frac{1}{\sqrt{x^2+y^2+z^2}}+\frac{w_c}{2}(xP_y-yP_x)+\frac{w_c^2(x^2+y^2)}{8}+f(x\,\cos\omega_f t+y\,\sin\omega_f t), \tag{1}$$

where the magnetic field is taken to lie along the positive z direction. In Eq. (1) ω_c is the cyclotron frequency, ω_f is the CP field frequency, and f is the electric field strength. Going to a frame rotating with the CP frequency ω_f, it is possible to eliminate the explicit time dependence in Eq. (1), producing the Hamiltonian [1]

$$\mathcal{H}=\frac{1}{2}(P_x^2+P_y^2+P_z^2)-\frac{1}{\sqrt{x^2+y^2+z^2}}-\left(\omega_f-\frac{w_c}{2}\right)(xP_y-yP_x)+\frac{\omega_c^2(x^2+y^2)}{8}+fx, \tag{2}$$

where x, y, and z are assumed to refer to the rotating frame. Now, due to the fact that trajectories with initial conditions $z=P_z=0$ remain always in the x-y plane, we focus our attention on the planar (2D) model. The corresponding 2D Hamiltonian takes the form

$$\mathcal{H}=\frac{1}{2}(P_x^2+P_y^2)-\frac{1}{\sqrt{x^2+y^2}}-\left(\omega_f-\frac{\omega_c}{2}\right)(xP_y-yP_x)+\frac{\omega_c^2(x^2+y^2)}{8}+fx. \tag{3}$$

We note that when $\omega_f=0$ (static electric field) the problem reduces to the planar hydrogen atom subjected to crossed electric and magnetic fields [9] and when $\omega_c=0$ the problem reduces to that of an orbiting dust particle under radiation pressure [10]. In order to examine the dynamics, it is convenient to scale coordinates and momenta according to

$$x'=\omega_c^{2/3}x,\quad y'=\omega_c^{2/3}y,\quad P_x'=\omega_c^{-1/3}P_x,\quad P_y'=\omega_c^{-1/3}P_y.$$

After dropping the primes, the Hamiltonian (3) converts to the form

$$\mathcal{K}=\frac{\mathcal{H}}{\omega_c^{2/3}}=\frac{1}{2}(P_x^2+P_y^2)-\frac{1}{\sqrt{x^2+y^2}}-\left(\Omega-\frac{1}{2}\right)(xP_y-yP_x)+\frac{1}{8}(x^2+y^2)+\mathcal{F}x, \tag{4}$$

where $F=f/\omega_c^{2/3}$, $\Omega=\omega_f/\omega_c$, and the dynamics depends only on the three parameters $\mathcal{K}$, Ω, and F. It is worth to note that the Hamiltonian (4) defines an integrable system in the cases $\Omega=\frac{1}{2}$ [11] and $\mathcal{F}=0$ [10,12].

We can split the Hamiltonian (4) as the sum $\mathcal{K}=\mathcal{K}_0+\mathcal{K}_1$ with

$$\mathcal{K}_0=\tfrac{1}{2}\left(P_x^2+P_y^2\right)-\frac{1}{\sqrt{x^2+y^2}},$$

$$\mathcal{K}_1=-(\Omega-\tfrac{1}{2})(xP_y-yP_x)+\tfrac{1}{8}(x^2+y^2)+\mathcal{F}x,$$

where the first term $\mathcal{K}_0$ defines a pure Keplerian system. At this point, for negative values of $\mathcal{K}_0$ (bounded orbits), a normalization in the usual sense (cf., e.g., [13]) allows one to reduce the planar CP×**B** problem to a dynamical system with one degree of freedom. As Deprit *et al.* [7] did for the Stark quadratic Zeeman effect, we perform the normalization in the Delaunay variables $(I_1,I_2,I_3\phi_1,\phi_2,\phi_3)$.[1] However, since we are treating with a 2D system, we use the planar Delaunay variables (I_2,I_3,ϕ_2,ϕ_3), where I_2 is the magnitude of the orbital angular momentum, I_3 is the principal action, ϕ_2 is the argument of the perinucleus, and ϕ_3 is the mean anomaly. The Delaunay normalization [16] is a canonical transformation

$$(I_2,I_3,\phi_2,\phi_3)\rightarrow(I_2',I_3',\phi_2',\phi_3')$$

that converts $\mathcal{K}$ into a function that does not depend on the mean anomaly ϕ_3'. To first order, we get $\mathcal{K}'$ simply by averaging the function $\mathcal{K}$ over the mean anomaly ϕ_3. Carrying out this operation and dropping the primes in the averaged variables, the normalized Hamiltonian comes out as the sum

$$\mathcal{K}'=\mathcal{K}_0'+\mathcal{K}_1',$$

$$\mathcal{K}_0'=-\frac{1}{2I_3^2},$$

$$\mathcal{K}_1'=-(\Omega-\tfrac{1}{2})I_2+\tfrac{3}{16}e^2I_3^4-\tfrac{3}{2}\mathcal{F}eI_3^2\cos_2,$$

where $e=\sqrt{1-I_2^2/I_3^2}$ is the eccentricity of the Keplerian electronic orbits. This normalized Hamiltonian, in the limit $\Omega=\frac{1}{2}$, falls into the category described by Farrelly and Uzer [12].

Because ϕ_3 is ignorable in $\mathcal{K}'$, the momentum I_3 is an integral of the motion. Moreover, $\mathcal{K}_0'$ may be neglected and the normalized Hamiltonian reduces to

$$\mathcal{K}'=\mathcal{K}_1'=-(\Omega-\tfrac{1}{2})I_2+\tfrac{3}{16}e^2I_3^4-\tfrac{3}{2}\mathcal{F}eI_3^2\cos\phi_2. \tag{5}$$

We do not enter into the details of the algebraic operations involved in constructing the normalized Hamiltonian other than noting that they were executed with the symbolic processor MATHEMATICA [17].

It is worth noting that the maps of $\mathcal{K}'$ on the cylinders (ϕ_2,I_2) do not cover the entire phase space because they exclude the points $e=0$ (circular orbits) at which the argument of perinucleus ϕ_2 is not defined. This singularity, as Deprit and Ferrer show [18], disappears when the system is handled in the variables

$$u=e\,\cos\phi_2,\quad v=e\,\sin\phi_2,\quad w=\pm\sqrt{1-e^2}=\pm\frac{I_2}{I_3}, \tag{6}$$

where we recognize the Cartesian components of the Runge-Lenz vector and the norm of the angular momentum I_2 divided by I_3. In this new map (u,v,w), since

$$u^2+v^2+w^2=1,$$

the phase space consists of a unit radius sphere. In these coordinates, the points with $w>0$ $(I_2>0)$ stand for Keplerian ellipses traveling in a direct (prograde) sense, while those points with $w<0$ $(I_2<0)$ represent Keplerian ellipses traveling in a retrograde sense. Moreover, any point in the equatorial circle $w=0$ $(I_2=0)$ corresponds to a straight line passing through the origin. Finally, the north (south) pole corresponds to circular orbits $(e=0)$ traveling in a direct (retrograde) sense.

In coordinates (u,v,w) the Hamiltonian $\mathcal{K}'$ becomes the function

$$\mathcal{K}'=\tfrac{3}{16}I_3^4-\tfrac{3}{16}I_3^4w^2-(\Omega-\tfrac{1}{2})I_3w-\tfrac{3}{2}\mathcal{F}I_3^2u, \tag{7}$$

[1]For a more complete definition see [14]; the notations adopted in this paper are those of [15].

The first term on the right-hand side may be neglected because it is a constant. After an overall multiplication of Eq. (7) by $-3I_3^4/8$ and defining the new parameters (P,Q),

$$P=\frac{8}{3I_3^3}\left(\Omega-\frac{1}{2}\right), \quad Q=\frac{4}{I_3^2}\mathcal{F}, \tag{8}$$

we can write Eq. (7) as

$$\mathcal{K}'=\tfrac{1}{2}w^2+Pw+Qu \tag{9}$$

and the normalized CP×**B** problem is regarded as a dynamical system represented by a biparametric quadratic Hamiltonian on the unit sphere $\mathcal{S}^2$. This class of Hamiltonians was studied by Lanchares and Elipe [19]. Taking into account the Liouville-Jacobi theorem and the Poisson brackets between variables (u,v,w),

$$[u,w]=w, \quad [v,w]=u, \quad [w,u]=v,$$

the equations of motion associated with $\mathcal{K}'$ are

$$\begin{aligned}\dot{u}&=(u;\mathcal{K}_1)=-v(P+w),\\ \dot{v}&=(v;\mathcal{K}_1)=u(w+P)-wQ,\\ \dot{w}&=(w;\mathcal{K}_1)=Qv.\end{aligned} \tag{10}$$

Equations (10) present the symmetry

$$(v,t)\rightarrow(-v,-t),$$

which indicates that the phase flow is time-reversal symmetric with respect to the plane $v=0$. Consequently, equilibria, if any, must lie in the plane $v=0$. The phase flow is determined for the most part by the equilibrium points and their stability. Equilibrium points are the local extrema of $\mathcal{K}'$ on $\mathcal{S}^2$, e.g., the roots of the system made on the right-hand side of Eq. (10) equal to 0 together with the relation $u^2+v^2+w^2=1$. With regard to the equilibrium points, stability, and bifurcations between equilibria as parameters (P,Q) evolve, Lanchares and Elipe [19] found a bifurcation curve given by the hypocycloid $P^{2/3}+Q^{2/3}=1$ and a bifurcation segment given by $(P=0,\ |Q|<1)$. In this way, when $P^{2/3}+Q^{2/3}>1$ (points outside the hypocycloid), there are only two isolated stable equilibria, while when $P^{2/3}+Q^{2/3}<1$, excluding the segment $(Q=0,\ |P|<1)$ (points inside the hypocycloid), there are four isolated equilibria (three stable and one unstable). Finally, when $(Q=0,\ |P|<1)$ the system presents two isolated stable equilibria and one infinite set of nonisolated equilibria in the minor circle $u^2+v^2=1-P^2$. In relation to the bifurcations between equilibria, Lanchares and Elipe showed that three types of bifurcations take place: a *teardrop* bifurcation when the hypocycloid is crossed, excluding the path $P=0$; a *pitchfork* bifurcation when the hypocycloid is crossed, following the path $P=0$; and an *oyster* bifurcation when, inside the hypocycloid, the axis $Q=0$ is crossed.

Substituting the values of parameters P and Q in the hypocycloid, we obtain the surface of bifurcation

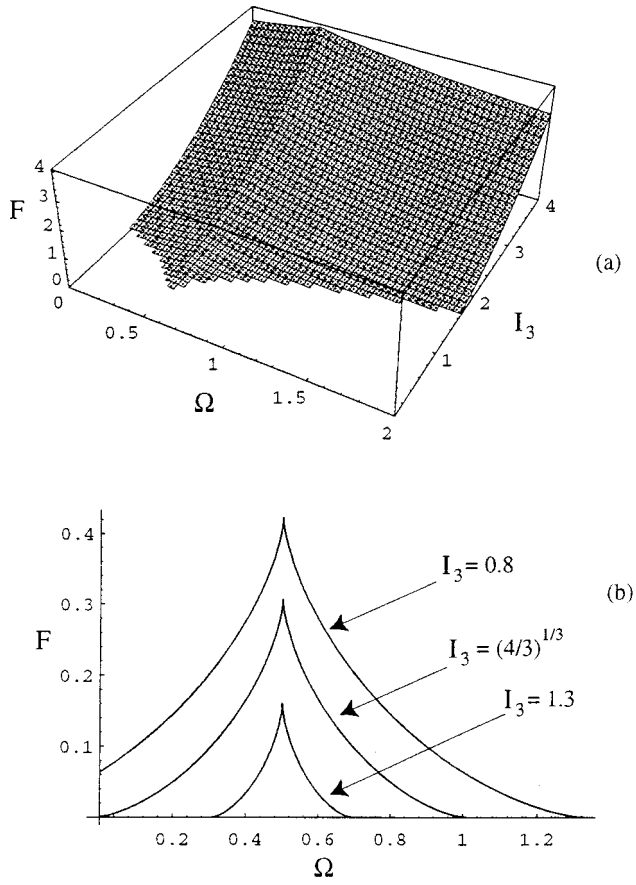

FIG. 1. (a) Surface of bifurcation. (b) Different intersection curves between Eq. (11) with planes of $I_3=$ const.

$$\left[\frac{8}{3I_3^3}\left(\Omega-\frac{1}{2}\right)\right]^{2/3}+\left[\frac{4}{I_2^3}\right]^{2/3}=1, \tag{11}$$

which is plotted in Fig. 1(a). Since $\Omega\geqslant 0$ and $F\geqslant 0$, this surface appears truncated by the planes $\Omega=0$ and $F=0$. As we observe in Fig. 1(b), the resultant curves of the intersection between Eq. (11) with planes of $I_3=$ const are also hypocycloids with an axis of symmetry located at $\Omega=\frac{1}{2}$. In other words, the qualitative dynamics exhibited is the same for all values of I_3. We also note that these hypocycloids appear also truncated at $\Omega=0$ (planar **E**×**B**) for values of $I_3>(\frac{4}{3})^{1/3}$ [see Fig. 1(b)]. This is because

$$|P|\leqslant 1, \quad \Omega\leqslant 0,$$

and Eq. (11) with $\Omega=0$ determines a bifurcation curve in the parametric plane $(I_3,\mathcal{F})$ for the planar **E**×**B** problem.

III. GLOBAL PHASE PORTRAIT AND BIFURCATIONS

Fixing a value of I_3, the hypocycloid (11) determines a partition in the parametric plane (Ω,F) in such a way that the phase portrait is different depending on which region (inside, outside, or on the hypocycloid) the parameters are. The traditional technique to build the phase portrait is to plot the trajectories by integrating numerically the equations of motion and has been used to produce the successive plots of Fig. 2. The figure shows the phase flow evolution of the

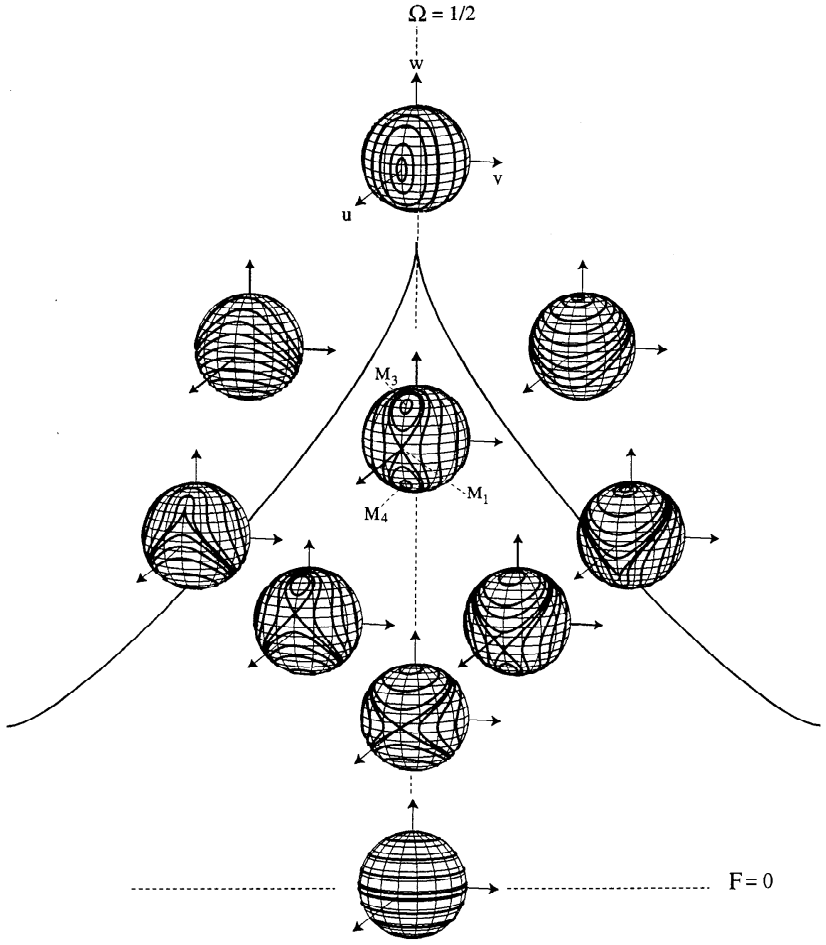

FIG. 2. Phase flow evolution of the system for $I_3=1$.

system for $I_3=1$. As we have already noted, the phase flow is symmetric with respect to the plane $v=0$ and the equilibria, when they exist, are named M_1, M_2, M_3, and M_4.

The sequence begins with the special value $\Omega=\frac{1}{2}$ (i.e., paramagnetic term absent) and $F=0.3$, i.e., inside the hypocycloid. Since $\Omega=\frac{1}{2}$ ($P=0$), the phase flow is symmetric with respect to the meridian $w=0$ and there are four equilibria. Only the equilibrium M_2, which is stable and located in $(-1,0,0)$, lies in the $u<0$ hemisphere. On the other hand, the other three equilibria are in the $u>0$ hemisphere: the points M_3 and M_4 are stable, while the remaining point M_1 is unstable and located in (1,0,0). As Ω increases (decrease), the symmetry with respect to the plane $w=0$ is broken and the unstable equilibrium M_1 migrates towards the stable equilibrium M_3 (M_4). Finally, equilibria M_1 and M_3 (M_4) coalesce when the parameters Ω and F are on the hypocycloid. As we observe in Fig. 2, the bifurcation that takes place is a *teardrop* bifurcation. Once the hypocycloid is crossed, the phase flow consists of circulations around M_4 and M_1 or around M_3 and M_1.

The bifurcation along the axis $\Omega=\frac{1}{2}$ is quite different. While for $F>\frac{1}{4}$ ($Q>1$) the phase flow consists of pure rotations around the u axis, when $F=\frac{1}{4}$ a pitchfork bifurcation appears and the stable equilibrium M_1 splits into three points: one unstable M_1 and two stable M_3 and M_4.

When Ω and $\mathcal{F}$ are inside the hypocycloid and $\mathcal{F}$ tends to zero while M_3 (M_4) tends to the north (south) pole, the two homoclinic orbits grow as $\mathcal{F}$ approaches zero. Finally, when $\mathcal{F}=0$, both homoclinic orbits meet one another along the minor circle $u^2+v^2=1-P^2$. This bifurcation is another example of an *oyster* bifurcation. In relation to $M_{3,4}$, they are located at $(0,0,\pm1)$. At this point, we have to remark that the presence of the minor circle of nonisolated equilibria is spurious: it is because the problem is treated in the frame of reference rotating with the CP frequency.

IV. ENERGY-LEVEL STRUCTURE

The above study of global phase portrait and bifurcations provides insight into the energy-level structure. In this way, when ($\Omega=\frac{1}{2},\mathcal{F}$) are inside the hypocycloid, there are two types of energy states corresponding to levels around $M_{3,4}$ (the so-called low-energy symmetrical vibrational motion [20–22] and levels around M_1 (the so-called high-energy rotational motion [20–22]). These two topological different kinds of states are separated by a separatrix passing through M_2. The separatrix is also a path along which tunneling occurs, lifting the degeneracy between vibrational states [21]. When the hypocycloid is crossed along the segment $\Omega=\frac{1}{2}$ (i.e., pitchfork bifurcation takes place), both classes of vibrational levels disappear and a new class of low-energy rotational states emerges.

The symmetry between the vibrational states is broken when ($\Omega\neq\frac{1}{2},\mathcal{F}$) are inside the hypocycloid. Accordingly, three classes of states result: two vibrational states around $M_{3,4}$ and a rotational state localized around M_1. When the hypocycloid is crossed (i.e., teardrop bifurcation occurs), one

class of vibrational levels disappears and the rotational states and a single class of vibrational states remain.

V. CONCLUSION

We have found that the normalized CP×**B** 2D problem presents a bifurcation surface in the space of parameters $(\Omega,\mathcal{F},I_3)$. In this way, the problem shows three kinds of bifurcations: the *pitchfork* bifurcation, the *teardrop* bifurcation, and the *oyster* bifurcation, depending on how the bifurcation surface is crossed. The phase flow evolution of the system was studied and a compact geometrical picture of the energy-level structure of the problem was provided.

ACKNOWLEDGMENTS

The authors thank Professor David Farrelly for his hospitality during a visit at the Department of Chemistry, Utah State University, Logan, as well as for his helpful comments. This work has been partially supported by University of La Rioja Projects Nos. 95TDA02JSI and 96PYB32VLB.

[1] E. Lee, A. F. Brunello, and D. Farrelly, Phys. Rev. Lett. **75**, 3641 (1995).
[2] C. W. Clark, E. Korevaar, and M. G. Littman, Phys. Rev. Lett. **54**, 320 (1985).
[3] A. Deprit, Celest. Mech. **1**, 12 (1969).
[4] K. R. Meyer, in *Computer Aided Proofs in Analysis*, edited by K. R. Meyer and D. S. Schmidt (Springer-Verlag, New York, 1991), pp. 190–210.
[5] A. J. Lichtenberg and M. A. Lieberman, *Regular and Stochastic Motion* (Springer-Verlag, Berlin, 1992).
[6] S. L. Coffey, A. Deprit, B. R. Miller, and C. A. Williams, Ann. (N.Y) Acad. Sci **497**, 22 (1986).
[7] A. Deprit, V. Lanchares, M. Iñarrea, J. P. Salas, and J. D. Sierra, Phys. Rev. A **54**, 3885 (1996).
[8] V. Lanchares, Ph.D. thesis, University of Zaragoza, 1993.
[9] T. Uzer and D. Farrelly, Phys. Rev. A **52**, R2501 (1995).
[10] A. Deprit, in *The Big-Bang and George Lemaitre*, edited by A. Berger (Reidel, Dordrecht, 1984), pp. 151–180.
[11] T. E. Dialynas and E. G. Floratos, Phys. Lett. A **228**, 363 (1997).
[12] D. Farrelly and T. Uzer, Celest. Mech. Dyn. Astron. **61**, 71 (1995).
[13] R. Abraham and J. E. Marsden, *Foundations of Mechanics* (Benjamin/Cummings, Reading, MA, 1980).
[14] B. Goldstein, *Classical Mechanics*, 2nd ed. (Addison-Wesley, Reading, MA, 1980).
[15] J. B. Delos, S. K. Knudson, and D. W. Noid, Phys. Rev. A **28**, 7 (1983).
[16] A. Deprit, Celest. Mech. **26**, 9 (1981).
[17] S. Wolfram, *Mathematica, A System for Doing Mathematics by Computer* (Addison-Wesley, New York, 1990).
[18] A. Deprit and S. Ferrer, Rev. Acad. Cienc. Zaragoza **45**, 111 (1990).
[19] V. Lanchares and A. Elipe, CHAOS **5**, 367 (1995).
[20] P. Cacciani, E. Luc-Koenig, J. Pinard, C. Thomas, and S. Liberman, Phys. Rev. Lett. **56**, 1467 (1986).
[21] T. Uzer, D. Farrelly, J. Z. Milligan, P. E. Raines, and J. P. Skelton, Science **242**, 42 (1991).
[22] D. Farrelly, T. Uzer, P. E. Raines, J. P. Skelton, and J. A. Milligan, Phys. Rev. A **45**, 4738 (1992).